Design of Wideband Hybrid QMSIW and Coupled-Line Filter by Direct-Synthesis Approach in the Bandpass Domain

Hanyu Tian[1], Yuandan Dong[2]
School of Electronic Science and Engineering,
University of Electronic Science and Technology of China (UESTC), China
[1]hanyutian@std.uestc.edu.cn, [2]ydong@uestc.edu.cn

***Abstract* — In this paper, a wideband hybrid bandpass filter using the quarter-mode substrate-integrated waveguide (QMSIW) and parallel-coupled lines is presented and discussed. For size- and radiation-reduction, the QMSIW cavity is folded and the striplines are shielded in an enclosed cavity. First, the working mechanism including the generation and coupling of the resonance is illustrated by the lumped-element equivalent circuits. Then, the filtering polynomials specified for a 5th-order general Chebyshev response are derived from the synthesis methodology in the bandpass domain. And the initial dimensions of the proposed filter are obtained by applying the investigated direct mapping techniques between the polynomials and the values of the lumped elements. A transmission zero (TZ) introduced by the folded QMSIW is also taken into consideration in the synthesis process. Finally, a multilayer filter prototype is designed, simulated and implemented following the synthesis procedure. The proposed hybrid filter shows the advantages in terms of wide bandwidth (61.8 % 3-dB FBW), low insertion loss (0.76 dB), high rejection level (-60 dB @ 1.5 f_0), low radiation and compact size (0.14 λ_g × 0.14 λ_g), etc.**

***Keywords* — Direct synthesis technique (DST), filter, hybrid structure, quarter-mode SIW (QMSIW), shielded stripline, wideband filter.**

I. Introduction

Wideband filters with low loss and deep rejection are highly demanded components for ultra-wideband systems to achieve high-quality data transmissions. Up to now, many planar bandpass filters with wide bandwidth have been reported. For example, an ultra-wideband microstrip filter with a fractional bandwidth of 124.6% was designed using shorted coupled-lines and transversal transmission line in [1], but the selectivity is poor due to the limited filtering orders. And a triple-mode quarter mode substrate-integrated waveguide (QMSIW) bandpass filter was proposed in [2]. The loss of the filter is reduced due to the *Q*-improvement of the cavity, but the harmonics appear close to the passband, and the footprint of the SIW filter is also large.

Recently, filters with the hybrid realization of resonator forms have been proposed and studied [3]–[6]. Among them, hybrid SIW and microstrip/stripline filters exhibit some attractive features, including reduced size, wide stopband, and flexible coupling schemes. A 4th-order bandpass filter composed of two SIW cavities and a pair of microstrip-based uniform-impedance resonators is reported by Zhu *et al.* [3]. Four transmission poles are elaborately coupled and the higher-order modes are suppressed. However, the bandwidth is narrow, and the size of the filter is still large compared with

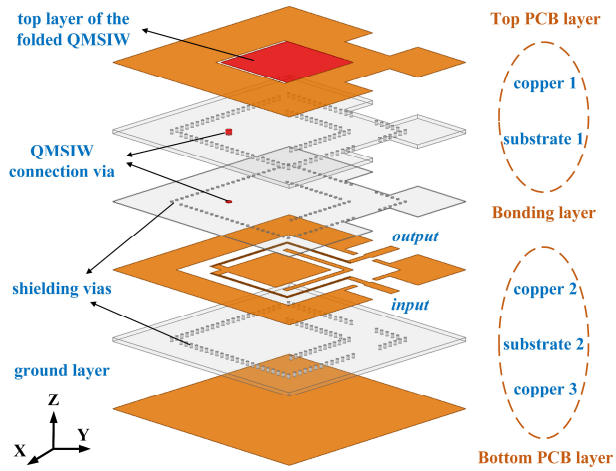

Fig. 1. 3D-exploded view of the proposed wideband hybrid filter.

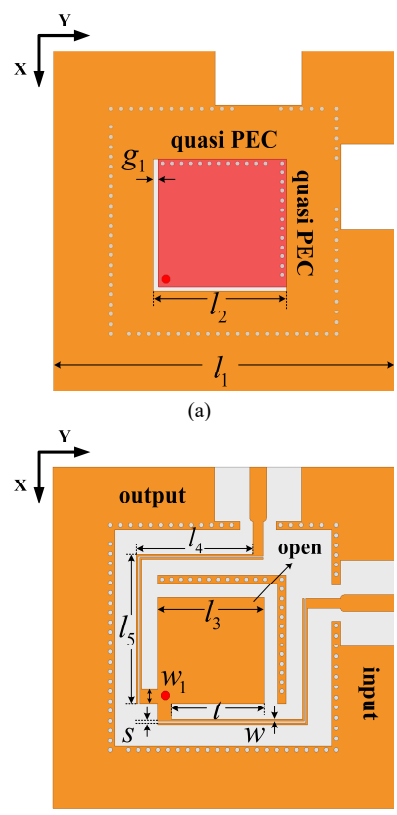

Fig. 2. Top views of (a) copper 1, and (b) copper 2.

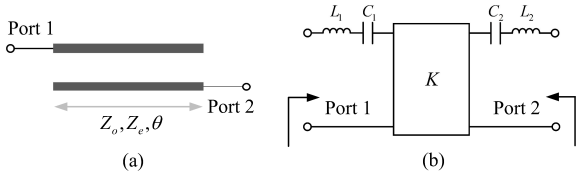

Fig. 3. (a) The parallel-coupled double-line section, and (b) Its equivalent circuit.

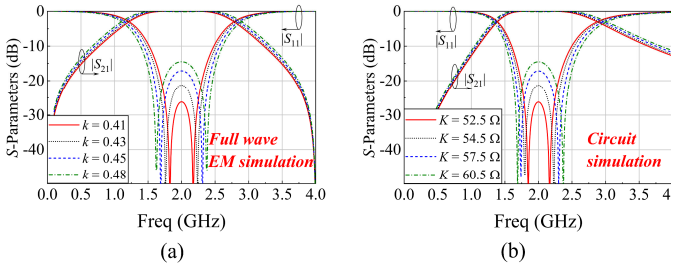

Fig. 4. *S*-parameters of the parallel-coupled two-line section with f_0 = 2 GHz based on: (a) Distributed-element circuit, and (b) Lumped-element circuit.

other planar configurations. In addition, the coupling matrix approach adopted in the synthesis stage is a near-band approximation, which is not accurate enough for wideband applications. Therefore, developing and synthesizing hybrid bandpass filters with wide bandwidth, low loss and reduced size is still a significant and challenging work.

In this study, a wideband hybrid filter based on the folded-QMSIW-cavity loaded parallel-coupled lines is investigated. The synthesis technique in the bandpass domain as well as the direct mapping approach are applied to develop the design procedure. The dimensions of the filter could be directly determined once the desired filtering specifications are given. An additional TZ is generated by the virtual short-circuit point of the QMSIW, which enhances the 2nd-harmonic suppression. And the proposed filter is packaged in a multilayer configuration, with the stripline fully shielded in the substrate-integrated cavity. It reduces the radiation and enhances the anti-interference capability. Finally, a 5th-order general-Chebyshev bandpass filter with a center frequency of 1.92 GHz, 3-dB bandwidth of 1.2 GHz, and an in-band return loss under 30 dB is synthesized, fabricated, and measured for demonstration and verification.

II. Filter Topology and Equivalent Circuit

The 3D-exploded view of the proposed 5th-order hybrid filter is shown in Fig. 1, which is composed of two PCBs, assembled by a 0.078-mm-thick bonding layer. And the top views of coppers 1 and 2 are depicted in Figs. 2(a) and (b), respectively. A pair of identical parallel-coupled two-line sections with the width of *w* and the space of *s* are connected to the folded QMSIW cavity on copper 2, which are meandered and fully shielded. The quasi Perfect-E condition (PEC) is formed by the metalized vias through coppers 1 to 3, as shown in Fig. 2(a). And the open end of the QMSIW is folded into copper 2, as indicated in Fig. 2(b). The two parts of the QMSIW are connected by a 0.8-mm-diameter red via.

Firstly, the distributed- to lumped-element equivalences of the parallel-coupled lines and the folded QMSIW resonator are applied to establish the equivalent circuit of the proposed

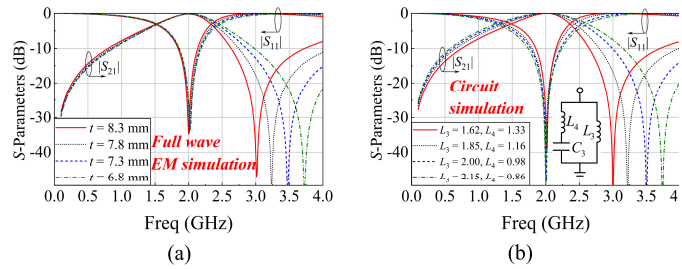

Fig. 5. *S*-parameters of the folded QMSIW with f_0 = 2 GHz. (a) Distributed-element circuit under different *t*. (b) Lumped-element circuit under different L_3 and L_4 (units: nH).

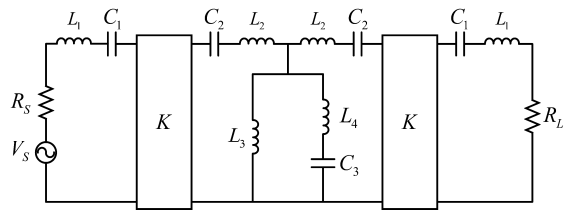

Fig. 6. Equivalent lumped-element circuit of the proposed hybrid filter.

filter. When the electrical length θ approximates to 90°, the parallel-coupled double-line section with the odd- and even-mode characteristic impedances of Z_o and Z_e could be equivalent to a 2nd-order lumped-element bandpass-filter circuit as shown in Figs. 3(a) and (b). The lumped element approximation consists of two serial *LC* resonators and a frequency-invariant impedance inverter with a reference impedance of *K*. The equivalent equations are:

$$K = \frac{(Z_e - Z_o)}{2\sin\theta} \tag{1}$$

$$L_1 = L_2 = \frac{\pi \cdot (Z_e + Z_o)}{8\omega_0} \tag{2}$$

$$C_1 = C_2 = \frac{8}{\pi\omega_0 \cdot (Z_e + Z_o)} \tag{3}$$

where ω_0 is the angular center frequency of the desired passband. The scattering parameters of the parallel-coupled double-line section and its equivalent lumped-element circuit under different coupling coefficients ($k = (Z_e - Z_o) / (Z_e + Z_o)$) are shown in Figs. 4(a) and (b), respectively. It is noted that the roll-off rate of $|S_{21}|$ in the full-wave EM simulation is higher than that in the lumped-element circuit model simulation because there are periodical TZs at mf_0 (*m* is a non-zero even number) due to the distinctive property of the distributed parallel-coupled line element, which could be modelled by higher-order approximation.

The folded QMSIW resonator could also be equivalent by the lumped-element *LC* circuits. The inductance from the feeding point to the quasi-PEC boundary is modeled by the shunted inductor L_3, with the connection via's (the red circle in Fig. 2(b)) inductance included. And the propagation path from the feeding point to the open-circuit end is equivalent to inductor L_4, grounded by a serial capacitor C_3. The resonant frequency f_1 and the position of the TZ (f_{zero}) of the circuit are:

$$f_1 = 1/2\pi\sqrt{(L_3 + L_4)C_3} \tag{4}$$

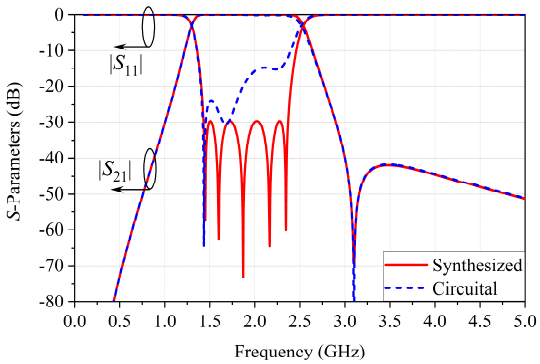

Fig. 7. *S*-parameters of the synthesized and circuital response.

$$f_{zero} = 1/2\pi\sqrt{L_4 C_3} \tag{5}$$

In the distributed-element model, the resonant frequency is determined by the dimensions of the cavity, while the bandwidth is controlled by the feeding position *t*. Larger relative bandwidth could be realized by decreasing *t*, corresponding to the process of enlarging L_3 and reducing L_4. Figs. 5(a) and (b) show the *S*-parameters of the QMSIW resonator and its equivalent circuit, respectively. A TZ is introduced when the electrical length from the feeding position to the open-circuited end equals 90°, modeled by the serial resonance of L_4 and C_3. Finally, the equivalent lumped-element model of the proposed 5th-order hybrid filter could be derived as shown in Fig. 6.

III. Synthesis Procedure and Demonstration

The synthesis procedure of the proposed 5th-order filter includes four steps:

1) Derive the filtering polynomials of the specified general Chebyshev response according to the DST process in the bandpass domain [7].

2) Yield the normalized transmission matrix ([ABCD] matrix) based on the filtering polynomials.

3) Calculate the values of the lumped elements in Fig. 6 by direct mapping approach.

4) Realize the lumped-element components by the distributed-element circuit based on the equivalence equations (1)-(3) and the relations between the QMSIW cavity and its equivalent models.

5) Optimize the filter using full-wave simulation tools until it meets the requirement.

For demonstration, a 5th-order wideband hybrid filter with a center frequency f_0 of 1.92 GHz, the 30-dB maximum-return-loss bandwidth of 0.95 GHz is synthesized. Two critical modifies are investigated to extend the DST method discussed in [7]:

a) The formula to calculate the transfer polynomial should be modified as:

$$\varepsilon \cdot P(\bar{s}) = P_0(\bar{s}) = \bar{s}^{2N_p} \cdot \prod_{k=1}^{N_m} (\bar{s}^2 - \bar{s}_{zk}^2) \tag{6}$$

, where $P(\bar{s})$ is the transfer polynomial, and ε could be determined by the specified ripple at the edge frequency of the passband.

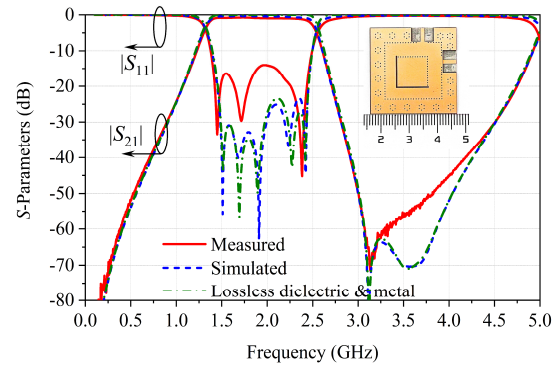

Fig. 8. *S*-parameters of the simulated and measured response.

Table 1. Performance comparison with recently published works.

Ref.	Size (λ_g^2)	f_0 (GHz)	FBW (%)	IL (dB)	Suppression
[1]	0.23 × 0.36	7.3	124.6	1.0	-15 dB @ 2.5f_0
[2]	0.88× 0.88	4.67	38	0.74	-10 dB @ 1.7 f_0
[3]	0.54 × 0.93	10.11	11.7	1.22	-20 dB @ 2.9f_0
[5]	0.71 × 3.21	9.25	44	1.2	-40 dB @ 1.3f_0
[6]	0.62 × 0.62	10	22.7	1.2	-36 dB @ 2.0f_0
Prop.	**0.14 × 0.14**	**1.925**	**61.8**	**0.76**	**-60 dB @ 1.5f_0**

Ref.: reference, IL: insertion loss. Prop.: proposed.

b) The number of the TZs at the origin (f = 0) could be an integer multiple of 0.5 (e.g., 0.5, 1, 1.5, 2…), and the remaining TZs except the ones at finite frequencies are all located at the infinity.

Assigning 1 TZ at 3.12 GHz, 2.5 TZs at the origin, and 1.5 TZs at the infinity, the filtering polynomials from the modified DST are:

$$\begin{aligned} F(\bar{s}) &= 483 + 748\bar{s}^2 + 449\bar{s}^4 + 130\bar{s}^6 + 18\bar{s}^8 + s^{10} \\ P(\bar{s}) &= 0.25\bar{s}^5(9.61 + \bar{s}^2) \\ E(\bar{s}) &= 483 + 398\bar{s} + 912\bar{s}^2 + 529\bar{s}^3 + 603\bar{s}^4 \\ &+ 240\bar{s}^5 + 174\bar{s}^6 + 43.9\bar{s}^7 + 22.2\bar{s}^8 + 2.76\bar{s}^9 + s^{10} \end{aligned} \tag{7}$$

Then the transmission matrix is derived as:

$$\begin{aligned} &\begin{bmatrix} a & b \\ c & d \end{bmatrix} = \frac{1}{\bar{s}^5(9.61 + \bar{s}^2)} \begin{bmatrix} \bar{a} & \bar{b} \\ \bar{c} & \bar{d} \end{bmatrix} \\ &\bar{a} = \bar{d} = 1593\bar{s} + 2118\bar{s}^3 + 960\bar{s}^5 + 175\bar{s}^7 + 11\bar{s}^9 \\ &\bar{b} = 3863 + 6641\bar{s}^2 + 4208\bar{s}^4 + 1219\bar{s}^6 + 162\bar{s}^8 + 8\bar{s}^{10} \\ &\bar{c} = 657\bar{s}^2 + 617\bar{s}^4 + 176\bar{s}^6 + 15\bar{s}^8 \end{aligned} \tag{8}$$

Directly map the theoretical values of the elements with those of the [ABCD] matrix of the lumped-element circuit. And the values of the inductors and capacitors in Fig. 6 could be determined: $L_1 = L_2 = 5.71$ nH, $C_1 = C_2 = 1.31$ pF, $L_3 = 1.62$ nH, $L_4 = 1.01$ nH, $C_3 = 3.43$ pF. The synthesized and circuital responses are shown in Fig. 7. Good agreement is achieved, and the in-band ripple of the $|S_{11}|$ of the circuit is due to the truncation error when calculating the values of the elements. Following the equivalence relations (1)-(5), the initial dimensions of the proposed filter could be determined: Z_e = 126 Ω, Z_o = 51.8 Ω, $\theta = 90°$, f_1 = 1.91 GHz, f_{zero} = 3.12 GHz.

IV. Fabrication and Measured Results

For verification, the demonstrated filter is implemented by a multilayer PCB process. And the substrates 1 and 2 in Fig. 1 are 0.508-mm-thick Rogers RT/Duriod 5880 with a loss tangent of 0.0009 and a dielectric constant of 2.2. And the bonding layer is Megtron_3313_Laminate with a thickness of 0.0078 mm, a loss tangent of 0.002 and a relative permittivity of 3.71. The dimensions of the filter are: w = 0.16, w_1 = 1.25, s = 0.152, l_1 = 31.4, l_2 = 12.25, l_3 = 9.8, l_4 = 10.74, l_5 = 13.7, g_1 = 0.45, and t = 8.55 (unit: mm). And the simulated and measured results of the proposed filter as well as its photograph are shown in Fig. 8. A 5th-order general Chebyshev filtering response is achieved. And an extra TZ located at about 3.1 GHz is observed as expected. The measured center frequency is 1.925 GHz, and the 3-dB bandwidth is 1.19 GHz. The minimum insertion loss over the passband is 0.76 dB, with the SMA connector loss included. Due to the shielding structure, the radiation loss is significantly reduced. A filter sample with the identical dimensions under lossless dielectric and lossless conductor is also simulated, as shown in Fig. 8. Its maximum loss in the passband is only 0.05 dB, indicating that most of the radiation is eliminated.

To further highlight the merits of the synthesis-designed wideband hybrid filter, Table 1 lists a comparison between the proposed filter and other recently published works. Compared with the conventional microstrip filters, the rejection level and loss performance of the proposed filter is better, and it also takes up less footprint compared with the SIW and other hybrid designs. The proposed filter takes the advantages in terms of the wide passband, low radiation, high out-of-band rejection and compact size.

V. Conclusion

In this paper, a wideband hybrid bandpass filter using folded QMSIW cavity and parallel-coupled double-line sections is proposed and discussed. Its working principle is clearly illustrated by the equivalent lumped-element circuit. The design procedure is developed based on the direct synthesis technique and the direct mapping approach. The filtering polynomials of the specified filtering response are derived by the modified real-coefficient DST in the bandpass domain. And the values of the lumped-element circuit are calculated by simply mapping the [ABCD] matrices' elements. Initial dimensions are obtained and an optimization process is also conducted. The proposed multilayer filter exhibits the merits of size reduction, low radiation, low loss, wide passband, and deep out-of-band rejection. The synthesis methodology presented in this paper could be further extended to devise filters in other configurations, which effectively shortens the design time and simplifies the design procedures.

References

[1] W. Feng and W. Che, "Novel ultra-wideband bandpass filter using shorted coupled lines and transversal transmission line," *IEEE Microw. Wirel. Compon. Lett.*, vol. 20, no. 10, pp. 548–550, 2010.

[2] C. Jin and Z. Shen, "Compact triple-mode filter based on quarter-mode substrate integrated waveguide," *IEEE Trans. Microw. Theory Tech.*, vol. 62, no. 1, pp. 37–45, 2014.

[3] Y. Zhu and Y. Dong, "A novel compact wide-stopband filter with hybrid structure by combining SIW and microstrip technologies," *IEEE Microw. Wirel. Compon. Lett.*, vol. 31, no. 7, pp. 841–844, 2021.

[4] J.-K. Xiao, N. Zhang, J.-G. Ma, and J.-S. Hong, "Microstrip/coplanar waveguide hybrid bandpass filter with electromagnetic coupling," *IEEE Microw. Wirel. Compon. Lett.*, vol. 26, no. 10, pp. 780–782, 2016.

[5] P. Chen, L. Li, K. Yang, and Q. Chen, "Hybrid spoof surface plasmon polariton and substrate integrated waveguide broadband bandpass filter with wide out-of-band rejection," *IEEE Microw. Wirel. Compon. Lett.*, vol. 28, no. 11, pp. 984–986, Nov. 2018.

[6] Y. Zheng, Y. Zhu, Z. Wang, and Y. Dong, "Compact, wide stopband, shielded hybrid filter based on quarter-mode substrate integrated waveguide and microstrip line resonators," *IEEE Microw. and Wireless Compon. Lett.*, vol. 31, no. 3, pp. 245–248, Mar. 2021.

[7] F. Xiao, "Direct synthesis of general chebyshev bandpass filters in the bandpass domain," *IEEE Trans. Circuits Syst. Regul. Pap.*, vol. 61, no. 8, pp. 2411–2421, 2014.